24th IMEKO TC4 International Symposium
22nd International Workshop on ADC and DAC Modelling and Testing
IMEKO TC-4 2020
Palermo, Italy, September 14-16, 2020

Low Frequency Bias-Induced Impedance

Sioma Baltianski [1]

[1] *Wolfson Dept. of Chemical Engineering, Technion – Israel Institute of Technology, Haifa, Israel,* cesema@technion.ac.il

***Abstract* – The paper presents the previously unreported properties of current-carrying conductors in the low frequency region utilizing impedance spectroscopy. The studied objects have an additional low frequency impedance during the passage of an electric current. The bias-induced impedance (Z_{BI}) is noticeably manifested in the range of 0.01 - 100 Hz and has either capacitive or inductive nature or both types, depending on the bias level (current density) and material types. The experiments in this work were done using wires made of pure metals, alloys, and non-metal conductors, such as graphite rods. These objects showed the Z_{BI}-*effect* that distinguishes them from other objects, such as standard resistors of the same rating, in which this phenomenon does not occur. The Z_{BI}-*effect* was modeled by equivalent circuits. Understanding the nature of this effect can give impetus to the development of a new type of instruments in various fields.**

***Keywords* – bias-induced impedance, impedance spectroscopy, low frequency**

I. INTRODUCTION

The impedance of current-carrying conductors is well known and described [1, 2]. As an example, we give the behavior of the impedance of a silver conductor 0.5 m long and 0.25 mm in diameter. The initial experiment in Fig. 1 without bias (at *Vdc* = 0 V) represents a typical behavior of the real and imaginary parts of the impedance in the frequency range 1 MHz - 100 mHz. First, we use the full frequency range to verify the processes. Later, we will be interested in events only in the low frequency part of the spectrum. The initial and all subsequent experiments were carried out at the amplitude of the test signal *Vac* = 10 mV. This signal corresponds to a small signal approach. The view of graph results is quite trivial at zero bias. Three approximate frequency domains can be distinguished in this graph: the high frequency region (HF) of the spectrum *f* = 1 MHz - 100 kHz; the mid frequency region (MF) *f* = 100 kHz - 100 Hz and the low frequency region (LF): *f* = 100 Hz – 0.1 Hz.

In the HF region there is an increase of a real Re(*Z*) and imaginary Im(*Z*) part of impedance with increasing frequency. This part is well described by a parallel connection of resistance *Rp* and inductance *Lp* (Fig. 1).

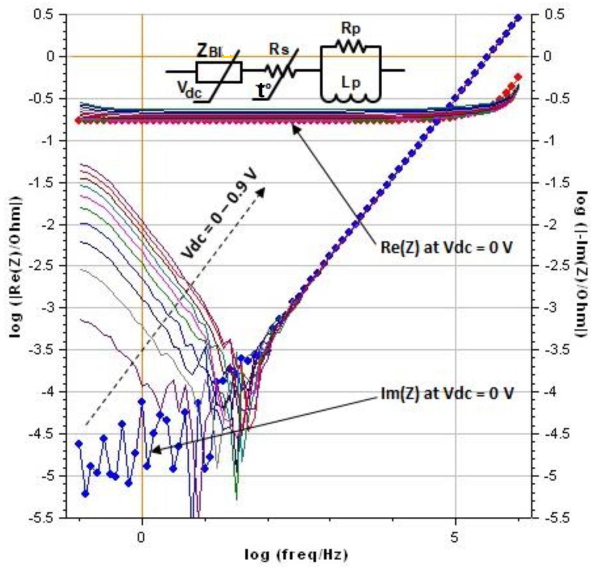

Fig. 1. Re*(Z) and* Im*(Z) of the silver wire at Vdc=0 – 0.9* V *with bias step 0.09* V*; length 500* mm *and diameter 0.25* mm*; frequency range 1* MHz *– 0.1* Hz

In the MF region, a constant value of Re(*Z*) is observed. Series resistance *Rs* must be added to the model. A linear decrease in the imaginary component occurs with a decrease in frequency (log-log scale). The relative noise level increases at the same time. This noise is natural and associated with the measuring system capabilities. The LF part of the spectrum at *Vdc* = 0 V demonstrates the constancy of Re(*Z*) and the strong noise of Im(*Z*). This area is not informative for interpretation using the imaginary part of the impedance. Measurements were made using a Faraday cage to improve the signal-to-noise ratio.

In this simple model, the specific resistance of the conductor determines the series resistance *Rs*. Mainly the length of the conductor determines the inductance *Lp*. The parallel resistance *Rp* that is connected to the inductance characterizes the active loss in the conductor due to the skin effect at high frequencies. The experimental values at zero bias correspond to the expected values and are quite common.

The situation changes significantly when measurements are taken under bias. The experimental characteristics are shown in the same Fig. 1 at biases *Vdc* = 0.09 - 0.18 V. The increment of bias was 0.09 V and the measuring test signal was the same: *Vac* = 10 mV. The HF and the MF imaginary part of the impedance does not change with bias. However, the LF part changes considerably. This response can be reflected by including an additional non-linear impedance Z_{BI} (Fig. 1). A corresponding increase of the real part of the impedance occurs in the considered region, which meets the Kramers–Kronig relationships [3]. Besides, we observe a monotonic change in the real component of the impedance in the entire frequency range (the model element *Rs*). This change is caused by a shift in the temperature of the conductor due to biases. The model indicated in the Fig. 1 is intuitive, but it well describes and fits the object under study in the specified frequency range.

The phenomenon of bias sometimes is difficult to detect because experimental data are often on the limit of the sensitivity of measuring instruments, namely, limitations on phase measurement with a high value of the loss tangent. Potentiostat/Galvanostat Biologic SP240 was used as a measuring instrument. In doubtful cases, data were verified using the Potentiostat/Galvanostat Gamry Reference 3000. A Biologic's contour plot defines an error not more than 0.3% and 0.3° in the desired measuring range. Thus, the experimental data in Fig. 1 is reliable. Moreover, in this case, we are interested in relative changes in the impedance components.

A homemade four-wire sample holder was used to connect the samples under test (SUT). We used standard not wire wound resistors as references to verify measuring results and estimate artifacts. This phenomenon was not observed when dealt with standard resistors of the same rating as SUT.

The impedance change in the LF region can be caused not only by bias using direct current but also by alternating current – by a large amplitude test signal at zero bias. It should be emphasized that in this work, we use a small signal approach in which a change in the LF impedance is not observed at zero bias. Thus, the occurrence of the additional impedance in the LF region will be determined solely by the level of bias. This physical phenomenon is named here as a bias-induced impedance (Z_{BI}-*effect*).

II. SYSTEMATIZATION OF THE EXPERIMENTAL RESULTS

We studied pure metals: nickel, copper, silver, tungsten, platinum, gold; alloys: constantan, nichrome, manganin; non-metals - graphite rods. Although the frequency scan began from 1 MHz toward low frequencies, the analysis of the results has carried out only for the LF part of the spectrum, where the Z_{BI}-*effect* was manifested.

According to the type of Z_{BI}-*effect*, all studied materials divided into three groups: (i) the Z_{BI}-*effect* has a capacitive nature, (ii) - an inductive nature, and (iii) - mixed when both types of reactance occur. Table 1 summarizes the properties of the investigated materials. Below are the experimental characteristics of one of the representatives of each group.

Table 1. Systematization of the investigated materials by the nature of Z_{BI}-effect

Type of conductors	Pure metals	Alloys	Non-metals (Graphite)
Nature of Z_{BI}-*effect*	Capacitive	mixture: Capacitive and Inductive	Inductive

A. Pure metals

We find significant changes in the behavior of the imaginary part of the impedance after a critical frequency of about 30 Hz (resonance point) when applying bias, Fig. 1. The inductive nature of reactance sharply changes to a capacitive nature from this point to the direction of LF. We see a monotonic change in the imaginary and real component of the impedance, depending on the applied bias. Changes in the real part of impedance in the mid frequency region also take place but this is due to a change in the temperature of the conductor upon bias. For example, with a maximum bias of 0.9 volts for this experiment and a conductor resistance of about 0.23 Ω, the current flowing through the conductor will be approximately 3.9 A. The power dissipation will be approximately 3.5 W, which will lead to certain heating of the conductor and consequential increase in its resistance. Fig. 2 shows a Nyquist graph of the LF part of the same experiment, which is shown in Fig. 1.

At mid and high frequencies, there is no change in the behavior of the imaginary component of the impedance under the influence of bias. Henceforward, we will limit visualization within the LF part of experimental data in the form of Nyquist plots. Similar in appearance, but numerically different in values, the characteristics were obtained in studies of other pure metals: nickel, copper, tungsten, platinum, and gold.

B. Alloys

The impedance characteristics of alloys as a function of bias differ from pure metals. Manganin demonstrated the inductive nature of reactance at moderate bias. In our nichrome and constantan samples, the Z_{BI}-*effect* had both capacitive and inductive reactance. The nature of the reactance depends on the level of bias.

As an example, studies of a nichrome sample with a diameter of 0.1 mm and a length of 57 mm are presented, Fig. 3. The experiment was carried out using a bias in the range of 2.8 - 8.5 V in increments of 0.1 V.

The data were taken in the frequency spectrum 1 MHz - 0.1 Hz, but only the range of interest is presented here: 100 Hz - 0.1 Hz.

Three areas of bias have been identified. In the bias of 2.8–4.6 V, the capacitive nature of the reactance was observed. In the range of 4.6 - 6.7 V, the increasing portion

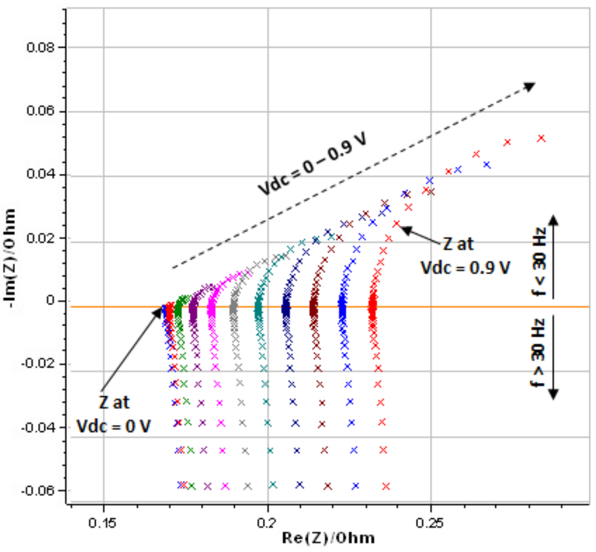

Fig. 2. Nyquist plot of silver wire at Vdc=0 – 0.9 V *with bias step 0.09* V*; length 500* mm *and diameter 0.25* mm

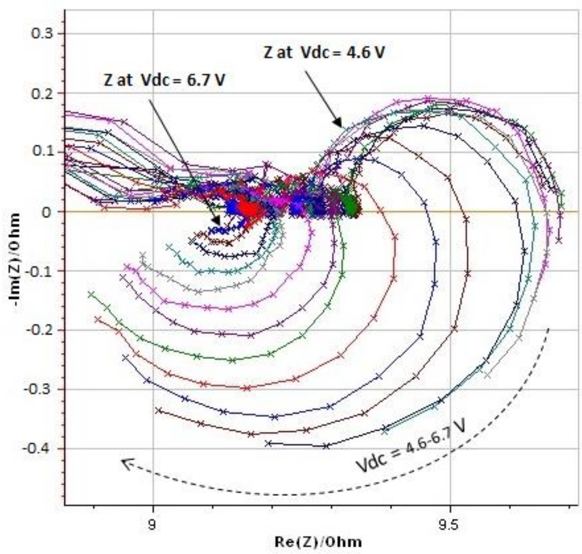

Fig. 3. Nyquist plot of nichrome wire at Vdc=4.6 – 6.7 V *with bias step 0.1* V*; length 57* mm *and diameter 0.1* mm

of the inductive nature of the reactance is added to the decreasing portion of the capacitive nature of the reactance. With a subsequent increase in bias, the reverse process occurs. Also, in the bias range of 6.7 - 8.5 V, the capacitive nature of the reactance was again demonstrated, the same as with a small bias. Fig. 3 shows a transient state when both types of reactance are present.

C. *Non-metals*

The measurements were carried out on graphite rods. Samples of various diameters have been investigated. Fig. 4 shows Nyquist plots of the impedance of the graphite rod 0.5 mm in diameter and 57 mm in length. The inductive nature of reactance has been demonstrated over the entire range of biases.

III. INTERPRETATION USING ELECTRICAL MODELS

First, we consider a simple case of interpreting experimental data related to pure metals in which the Z_{BI}-*effect* of capacitive nature is manifested. As an example, Fig. 5 presents a fitting result of the LF part of one of the experiments shown in Fig. 2, specifically at bias *Vdc* = 0.72 V. The fitting was carried out using the impedance model which consists of serial resistor *Rs* connected to parallel C_1 and R_1. The resistor *Rs* reflects specific resistance of the sample under test and its geometry. The resistance varies with the applied bias, which affects the temperature of the sample (see a right shift of characteristics in Fig. 2 with increasing bias). The parallel circuit C_1-R_1 exactly describes the Z_{BI}-*effect.* Fig. 5 shows a good fitting quality.

A similar approach for fitting can be used for materials in which the Z_{BI}-*effect* is purely inductive (Fig. 4) by using the *LR* - circuit.

The situation becomes more complicated in the case of a complex Z_{BI}-*effect* (Fig. 3). One of the possible electrical models that satisfactorily approximate the experimental data is embedded in Fig. 6.

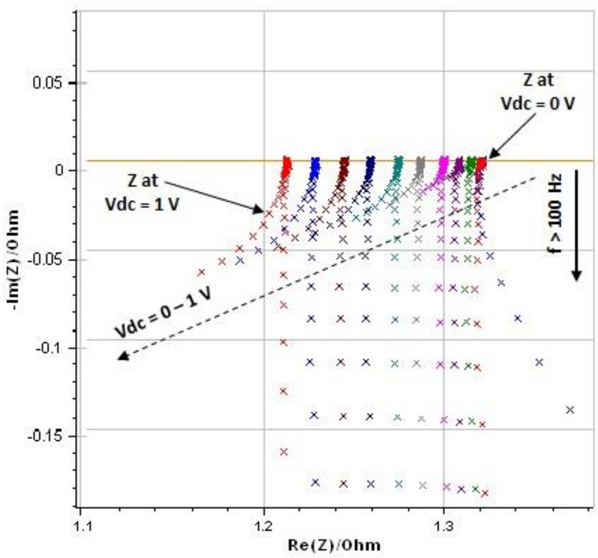

Fig. 4. Nyquist plot of graphite rod at Vdc=0 – 1 V *with bias step 0.1* V*; length 57* mm *and diameter 0.5* mm

A *system* function as a rational fraction [4] that corresponds to this model has the following form:

$$Z(s) = \frac{A_0 + A_1 \cdot s + A_2 \cdot s^2}{1 + B_1 \cdot s + B_2 \cdot s^2} \quad (1)$$

where: $s = j \cdot 2 \cdot \pi \cdot f$ *and* A_i , B_i unknown coefficients.

Although the system function uniquely approximates the experimental data, its coefficients are difficult to fill with a physical meaning. It is easier to do this using *circuit*

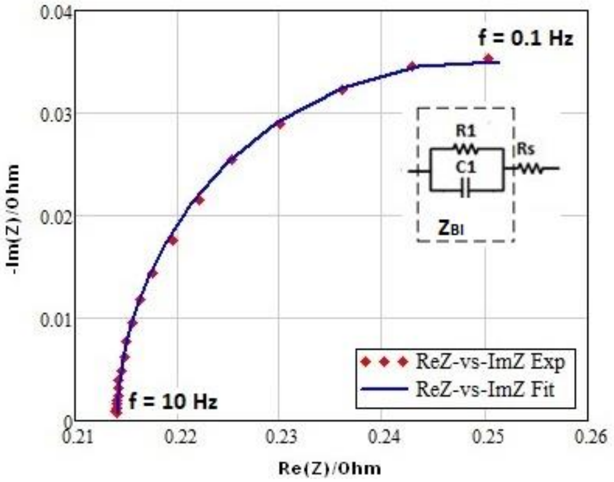

Fig. 5. Fitting result of LF part of data (f= 10 – 0.1 Hz*). Silver wire at Vdc=0.72* V*. Fit parameters: Rs=0.214* Ω*;* R_1*=0.07* Ω*;* C_1*=21.34* F

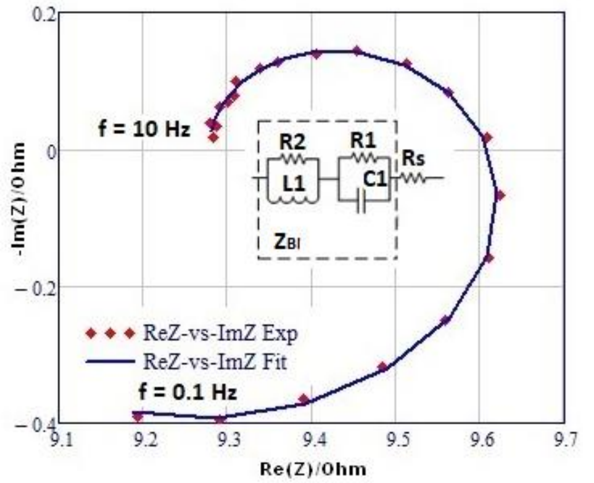

Fig. 6. Fitting result of LF part of data (f= 10 – 0.1 Hz*). Nichrome wire at Vdc=5.3* V*: Rs=8.261* Ω*;* R_1*=0.622* Ω*;* C_1*=0.373* F*;* R_2*=1.018* Ω*;* L_1*=1.091* H

functions which reflect the topology of the corresponding equivalent circuits [4]. The *circuit* function corresponding to the model in Fig. 6 has a form

$$Z(s) = R_s + \frac{R_1}{1+\tau_C \cdot s} + \frac{L_1 \cdot s}{1+\tau_L \cdot s} \qquad (2)$$

where: $\tau_C = R_1 \cdot C_1$; $\tau_L = L_1 / R_2$ and R_s, R_1, R_2, C_1, L_1, requested parameters from fitting .

The *system* function (1) covers several equivalent circuits. Fig. 6 represents one of the possible implementations. The results of fitting utilizing this circuit for one of the characteristics represented in Fig. 3, specifically at bias *Vdc* = 5.3 V, are given in Fig. 6. The selection of a suitable electrical model can be made empirically by iterating through the available set of models determined by the *system* function (1). To implement this process, experimental data can be approximated using an acceptable set of equivalent circuits and utilizing available fitting programs, such as LEVM [3].

Fig. 7 represents the dependencies of the model parameters versus bias of the silver wire corresponding to the data shown in Fig. 2. The capacitance C_1 increases exponentially with decreasing bias. This leads to a decrease in the contribution of the reactive component into the Z_{BI}-*effect*. At the same time, a monotonic decrease in resistance R_1 is observed. As a result, at zero bias, the Z_{BI}-*effect* demonstrated by the vanishingly small magnitude.

The resistance *Rs* reflects a change in resistivity as a function of temperature, which in turn depends on the flowing bias current. The temperature value (it got by utilizing resistivity) and power dissipation for this experiment shown in Fig. 8. Similar results, but differing in values, were obtained for other pure metals.

The graphite rod model behaves quite differently, Fig 9. First, the series resistance Rs decrease with bias due to a negative temperature coefficient (NTC). It distinguishes

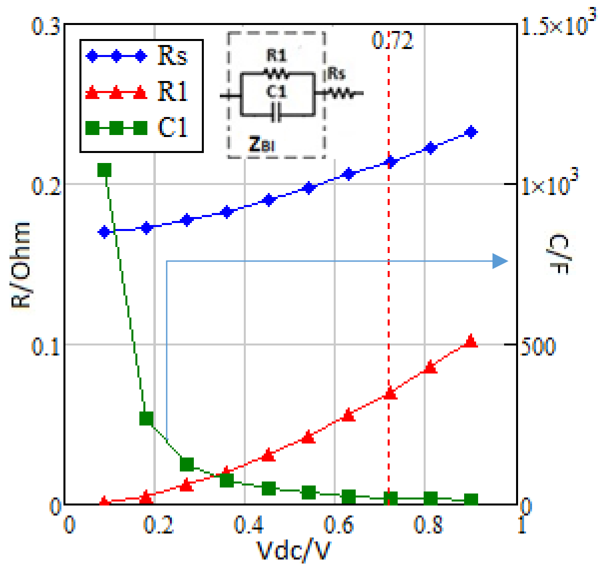

Fig. 7. Model parameters of silver wire as a function of bias - refer to the experiment data in Fig. 2

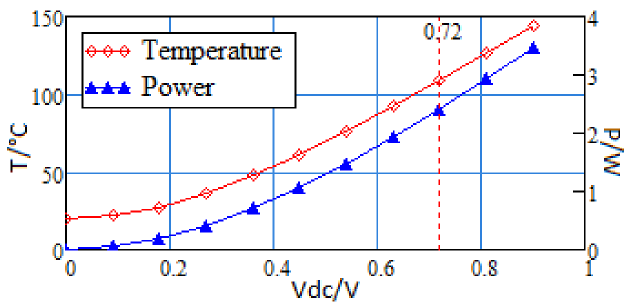

Fig. 8. Power dissipation and temperature of silver wire - refer to the experiment data in Fig. 2

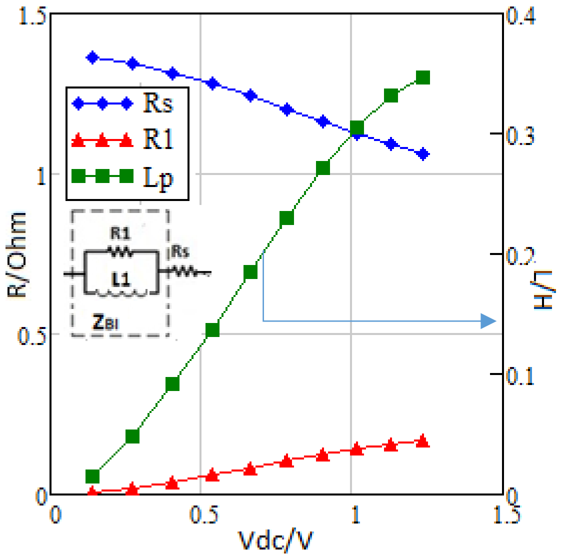

Fig. 9. Model parameters of graphite rod as a function of bias - refer to the experiment data in Fig. 4

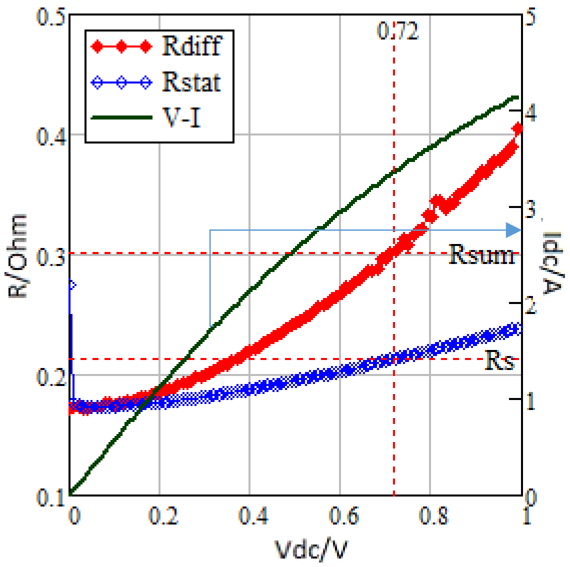

Fig.10. I-V – curve; static and differential resistance curves of silver wire with the same dimensions as in Fig. 2

them from metal in which there is a positive coefficient of resistance (PTC), see Fig. 7. Secondly, the inductance L_1, together with the parallel resistance R_1, decreases with decreasing bias. This nullifies the Z_{BI}-*effect* at zero bias.

The behavior of model parameters for alloys is more complex and is beyond the scope of this article. These studies are planned.

IV. CHECK OF THE DATA CONSISTENCY

Current-voltage characteristics were acquired on the same samples to check a data set for internal consistency. A sweep rate of 1 mV/s which is reasonable to our lowest frequency was selected. This speed allows getting quasi-static characteristics. Static and differential parameters, namely resistances, were calculated and compared with parameters obtained from impedance measurements.

The I-V characteristics of a silver sample are shown in Fig. 10. The parameters of the sample under test correspond to the parameters indicated in Fig. 2. The setup for I-V measurements was identical to the setup for impedance measurements.

Fig. 10 represents I-V curve, static resistance *Rstat*=*Vdc*/*Idc* and differential (dynamic) resistance *Rdiff*=d(*Vdc*)/d(*Idc*). A fairly well accordance was obtained between the model parameters extracted from impedance measurements and the parameters calculated from the current-voltage characteristics. The parameter *Rs* extracted from the impedance Z_{BI} and the *Rstat* extracted from the I-V well fit each other in an error of not more than 0.3%. The total resistance $Rsum=Rs+R_1$ found from the impedance measurements corresponds to the resistance *Rdiff* calculated from the I-V (Fig. 10). As an example, the bias point *Vdc* = 0.72 V was taken in Fig. 10 for indicating these correlations. It is corresponding to this bias point in Figures 5, 7 and 8.

The dependence of power dissipation $P_i + \Delta P$ on the influence of bias and the test signal at an operating point *i* will have the form

$$P_i + \Delta P = (V_i + \Delta V) \cdot (I_i + \Delta I) \qquad (3)$$

therefore, changes in power due to only the test signal is determined as

$$\Delta P = V_i \cdot \Delta I + I_i \cdot \Delta V + \Delta V \cdot \Delta I \qquad (4)$$

where: V_i, I_i - voltage and current at a working point and ΔV, ΔI – amplitudes of voltage and current of the test signal.

It can be seen (4) that with increasing bias the dissipated power caused by the test signal will increase. Hence, the temperature variation will increase, which will lead to an increase in a change of the resistivity by an influence of the test signal. This is an explanation of the magnification of the Z_{BI}-*effect* at all the experiments with increasing a bias.

V. DISCUSSIONS

The impedance of quite ordinary current conductors under bias in the low-frequency region demonstrates remarkable properties - named as Z_{BI}-*effect*. Now, the question of how to explain the occurrence of such significant reactive elements in the impedance models of the studied objects. In particular, the capacitance of pure metals reaches the order of farads (see Fig. 7). The inductance of graphite rods reaches about hundreds of millihenry (see Fig. 9). In reality, of course, such reactance does not exist in the studied objects. This phenomenon may be called as a “*phantom*” reactance.

This effect can be explained utilizing two necessary properties of the studied objects. The first is nonlinearity and the second one is inertia. The nonlinearity of current conductors is the second kind of nonlinearity (indirect). This property distinguishes them from objects of the first kind of nonlinearity (direct), such as p-n junctions or Schottky diodes.

In the case of the first kind, the nonlinearity reveals itself directly, without any delay. For the second kind of nonlinearity, it manifests itself due to a resistivity dependence on temperature. This is a factor of the studied material. The nonlinearity of the second kind has a significant delay. The bias sets a specific operating point. The test signal acts in the vicinity of this point. No matter how small the test signal is, it will change the temperature of the investigated object in the locality of the operating point with a certain delay. Consequently, the resistance of the material under investigation will cyclically change with the test signal.

Eventually, the resistance is modulated by the test signal. The difference between the phase of this modulation and the phase of the acting test signal determines the occurrence of *phantom* reactance. If the investigated object has a PTC property, a capacitive reactance arises. This is specific for pure metals or PTC thermistors. If the object under study has an NTC feature, then an inductive reactance arises. This is specific, for example, to graphite and NTC thermistors.

In terms of electrical measurements, impedance is properly defined only for systems satisfying stationarity [3]. In our case, we have a dynamic structure with one exception - the system changes cyclically and synchronously with an influence of the test signal. The amplitude and phase response depends on a frequency of the test signal. A purely active resistance, which changes are synchronously according test signal, but with a different phase relative to test signal, generates a reaction that looks like a complex resistance. As a result, a complex value will be estimated during the measurements as an impedance of the studied object.

Successive experiments revealed a significant feature. It turned out that the time constant following from the Z_{BI}-*effect's* model ($\tau = RC$ for PTC objects and $\tau = L / R$ for NTC objects) weakly depends on the applied bias. It is reasonable to assume that these time constants related to the time constant of the heat exchange between the object under study and the environment (air in our case). This implies the possibility of building specialized sensors to assess the thermal conductivity of various materials. This approach may be an alternative to the methods described in [5].

The experimental results obtained on the nichrome alloy motivates the appearance of additional ideas. In particular, both capacitive and inductive reactive components are observed at a bias Vdc = 5.3 V (Fig. 6) and in the areas close to it (Fig. 3) depending on the frequency of the test signal. Specifically, for Fig. 6 capacitive nature takes place in the frequency range of 10 Hz to 0.5 Hz, and inductive nature takes place in the range of 0.5 Hz to 0.1 Hz. Such effects are possible if we assume that the temperature coefficient of resistance (TCR) has *dynamic* properties. In other words, the TCR changes its character depending on the rate of temperature change. In turn, the rate of temperature variations at the selected operating point will be related to the frequency of the test signal. Therefore, in the higher frequency range will be observed a PTC-feature, in the lower frequency range will be observed an NTC-feature. This assumption was confirmed using I-V experiments with different sweep rates.

VI. CONCLUSIONS

The phenomenon of bias-induced impedance is described. This effect is most evident in the low frequency spectra of the reactive part of the impedance. The manifestation of the different nature of this issue is shown experimentally. The Z_{BI}-*effect* may be capacitive, inductive, or complex, which includes both types of reactance. The nature of the reactance depends on the type of test material. Pure metals showed capacitive reactance. Graphite rods showed inductive reactance. The alloys showed reactance of both types depending on the level of bias. The investigated objects can be attributed to the inertial nonlinear resistances.

The Z_{BI}-*effect* is caused by the thermal interaction between the conductor and the environment under the superposition of the bias combined with a test signal.

Relatively simple equivalent circuits have been found to describe the experimental data. Additional studies should be undertaken to better understand the behavior of alloys and other composites under the bias, especially unexpected (at least for the author) dynamic TCR properties.

REFERENCES

[1] The Self and Mutual Inductances of Liner Conductors. By Edward B. Rosa. Bulletin of the Bureau of Standards. U.S. Bureau of Standards. Vol.4. No2. Washington, September 15, 1907.

[2] Inductance Calculations: Working Formulas and Tables (Dover Phoenix Editions) Hardcover – March 29, 2004.

[3] E. Barsoukov, J. R. Macdonald (Eds.), Impedance Spectroscopy, Theory, Experiment, and Applications, 2nd Ed., New Jersey, John Wiley & Sons. Inc., 2005

[4] Baltianski, S.Sh. “Measuring the Parameters of Physical Objects by Identifying Electrical Models” Measurement Techniques, Vol. 43, No. 9, 2000, https://link.springer.com/article/10.1023/A:1026645722396

[5] Barsoukov E. and Jang J. H. and Lee H.., Thermal impedance spectroscopy for Li-ion batteries using heat-pulse response analysis, Journal of Power Sources, Vol. 109, pp 313-320, 2002